10522 *Biochemistry* **2009,** *48,* 10522–10532
DOI: 10.1021/bi901421t

BIOCHEMISTRY
including biophysical chemistry & molecular biology
Article

Biologically Active Sequences in the Mouse Laminin α3 Chain G Domain†

Shunsuke Urushibata,‡ Fumihiko Katagiri,‡ Shu Takaki,‡ Yuji Yamada,‡ Chikara Fujimori,‡ Kentaro Hozumi,‡ Yamato Kikkawa,‡ Yuichi Kadoya,§ and Motoyoshi Nomizu*,‡

‡*Laboratory of Clinical Biochemistry, School of Pharmacy, Tokyo University of Pharmacy and Life Sciences, Hachioji, Tokyo 192-0392, Japan, and* §*Department of Anatomy, Kitasato University School of Allied Health Sciences, Sagamihara, Kanagawa 228-8555, Japan*

Received August 14, 2009; Revised Manuscript Received October 6, 2009

ABSTRACT: The laminin α3 chain is mainly expressed at the skin, and its C-terminal G domain has a critical role in multiple biological functions. We screened for biologically active sites on the mouse laminin α3 chain G domain using 107 synthetic peptides on coated plates and conjugated to Sepharose beads with HT1080 human fibrosarcoma cells, HaCaT human skin keratinocyte cells, and human dermal fibroblasts (HDFs). Eleven peptides exhibited cell attachment activity with respect to the peptide-coated plates and/or peptide−Sepharose beads. MA3G28 (WTIQTTVDRGLL) strongly binds to HaCaT cells. Four peptides promoted PC12 cell neurite outgrowth. Heparin inhibited attachment of HDFs to eight peptides on the coated plates. In contrast, EDTA significantly inhibited attachment of HDFs to MA3G27 (NAPFPKLSWTIQ) and MA3G28 but had no effect on the attachment of the other peptides. HDF cells formed well-organized actin stress fibers and focal contacts with vinculin accumulation on MA3G27. Additionally, attachment of HDFs to MA3G27 was inhibited by anti-α6 and anti-β1 integrin antibodies, suggesting that MA3G27 promotes α6β1 integrin-mediated cell adhesion. MA3G57 (NQRLASFSNAQQS) exhibited cell attachment activity only in the peptide bead assay. MA3G57 conjugated to a chitosan membrane promoted HDF attachment and spreading with well-organized actin stress fibers. The anti-β1 integrin antibody partially inhibited attachment of HDFs to the MA3G57−chitosan membrane, suggesting that the MA3G57 site is involved in β1 integrin-mediated cell attachment. These active sites are likely important in the biological activities of the laminin α3 chain G domain and would be useful for the study of molecular mechanisms of laminin−receptor interactions.

Basement membranes, thin extracellular matrices, contain type IV collagen, nidogens, perlecan, and laminins (*1*). Laminins make up a family of glycoproteins that regulate diverse biological functions, such as cell adhesion, migration, proliferation, differentiation, wound healing, and tumor invasion (*2*). Currently, five α chains, three β chains, and three γ chains have been identified, and at least 16 different heterotrimeric isoforms are formed by various combinations of the three subunits depending on the tissue type and developmental stage (*3*, *4*).

Laminin-111 (α1β1γ1), which is the most extensively characterized isoform, was previously analyzed for biological activities using proteolytic fragments, recombinant proteins, and synthetic peptides (*5*−*10*). To identify the precise locations of biological active sites, we have previously screened cell adhesive sequences in laminin-111 using 673 overlapping synthetic peptides covering the whole molecule (*5*−*8*). Several active sequences that interacted with cell surface receptors in a peptide- and cell type-specific manner were identified, and many active sites were localized in the globular domain (G domain) of the α1 chain (*11*, *12*). The G domain in the C-terminal region of the α chain plays an essential role in the biological activities of basement membranes. The laminin G domain is composed of five tandem homologous modules (LG1−LG5), and each LG module contains approximately 200 amino acid residues (*13*). The biologically active sites in the G domain of the other α chains have been also identified using a similar approach (*12*). The active sequences are prominent sites for interaction with cellular receptors in the G domain (*13*).

The laminin α3 chain, a subunit of laminin-322, -311, -321, and -323, is mainly distributed in the skin and is important in tissue regeneration and wound healing (*14*, *15*). The secreted laminin α3 chain is generally cleaved between the LG3 and LG4 modules (*16*) and increases human keratinocyte cell migration activity in vitro (*17*). Using recombinant proteins, the LG1-3 module of the human laminin α3 chain is identified as being important for cell adhesion and motility via α3β1 and α6β1 integrins (*18*−*20*). Mutant mice with a defect in the *Lama3* gene have congenital epidermolysis bullosa with abnormal hemidesmosome formation, and lethality at the neonatal stage is observed (*21*). These results suggest that expression of the laminin α3 chain and its interaction with integrins are important for tissue integrity.

The human laminin α3 chain LG4 module interacts with cell surface syndecans, which are heparan sulfate-containing proteoglycans (HSPGs). The diverse biological functions of HSPGs depend on the sulfation patterns of the glycosaminoglycan side chains (GAGs) and developmental stage of the tissues. Previously, we reported that the A3G75aR peptide (NSFMALYLSKGR; human laminin α3 chain, residues 1412−1423),

†This work was supported by Grants-in-Aid for Scientific Research from the Ministry of Education, Cultures, Sports, Science and Technology of Japan to M.N. (17390024 and 17014081) and to K.H. (21750174).

*To whom correspondence should be addressed: Laboratory of Clinical Biochemistry, School of Pharmacy, Tokyo University of Pharmacy and Life Sciences, 1432-1 Horinouchi, Hachioji, Tokyo 192-0392, Japan. Phone and fax: +81-42-676-5662. E-mail: nomizu@toyaku.ac.jp.

 Published on Web 10/06/2009

containing the unique KGR sequence, is involved in heparin and syndecan-2 and -4 binding (*22*). The A3G756 peptide (KNSFMALYLSKGRLVFALG; human laminin α3 chain, residues 1412−1429), a longer sequence containing A3G75aR, induces cell adhesion (*22*), neurite outgrowth (*23*), and matrix metalloprotease-1 (MMP-1) secretion with the activation of p38 mitogen-activated protein kinase (MAPK) and extracellular signal-related kinase (Erk) via syndecan-2 and -4 (*24*, *25*). Fourteen β strands (strands A−N) in the crystal structure of the laminin α2 chain LG5 module (*26*) demonstrate that the A3G756 sequence is located on the connecting loop region between the E and F strands (*22*, *27*). Recently, we found that the loop structure of the E−F connecting region in the human laminin α3LG4 module is important for biological activity (*28*). These analyses have focused on the human laminin α3 chain LG4 module, but active sites in the entire laminin α3 chain G domain have not yet been identified.

Here, we analyzed the mouse laminin α3 chain G domain, whose sequence is 86% homologous with the human sequence. We prepared 107 overlapping synthetic peptides (MA3G1−MA3G107) covering the entire amino acid sequence to identify the biological active sites. Cell attachment assays with the synthetic peptides were performed with both peptide-coated plates and peptide-conjugated beads using three different cell lines. Neurite outgrowth activity was also evaluated on peptide-coated plates. The receptors involved in these biological activities were analyzed.

MATERIALS AND METHODS

Design of Peptides from the Mouse Laminin α3 Chain G Domain. One-hundred-seven overlapping peptides covering the mouse laminin α3 chain C-terminal G domain (positions 1626−2569) (*29*) were manually synthesized to identify biologically active sequences (Figure 1). Peptides were generally designed with a length of 12 amino acid residues and overlapped with neighboring peptides by four amino acids. If the N-terminal amino acid was either glutamate or glutamic acid, one amino acid was extended at the N-terminus to avoid pyroglutamine formation. Cysteine residues were omitted to prevent the influence of disulfide bonds.

Peptide Synthesis. All peptides were manually synthesized by the *N*-(9-fluorenyl)methoxycarbonyl (Fmoc) solid-phase method with a C-terminal amide as described previously (*11*). *N*,*N*-Dimethylformamide (DMF,[1] Kanto Chemical Co. Ltd., Tokyo, Japan) was used as a solvent during the synthesis. The following side chain-protected groups for each N^{α}-Fmoc amino acid were used: trityl for Asn, Cys, Gln, and His; *tert*-butyl for Asp, Glu, Ser, Thr, and Tyr; 2,2,5,7,8-pentamethyl-chroman-6-sulfonyl for Arg; and *tert*-butoxycarbonyl for Lys. The respective amino acids were condensed manually in a stepwise manner using diisopropylcarbodiimide and *N*-hydroxybenzotriazole on 4-(2′,4′-dimethoxyphenyl-Fmoc-aminomethyl)phenoxy resin (Rink amide resin, Merck, KGaA, Darmstadt, Germany). For deprotection of N^{α}-Fmoc groups, 20% piperidine in DMF was employed. The resulting protected peptide resins were deprotected and cleaved from the resin with a trifluoroacetic acid (TFA)/thioanisole/*m*-cresol/ethanedithiol/H_2O mixture (80:5:5:5:5, v/v) for 3 h at room temperature. The obtained crude peptides were precipitated and washed with diethyl ether and then purified by reverse-phase high-performance liquid chromatography (HPLC) on a Mightysil RP-18 GP 250-10 column (Kanto) using a gradient elution with water and acetonitrile containing 0.1% trifluoroacetic acid. Then, the desired peak was collected and lyophilized. The 107 peptides were manually synthesized and dissolved in Milli-Q water, but three peptides, MA3G11, MA3G21, and MA3G30, could not be purified because of their poor solubility. The 104 soluble peptides were used for the experiments. The purity and identity of the peptides were confirmed by analytical HPLC and electrospray ionization mass spectrometry at the Central Analysis Center, Tokyo University of Pharmacy and Life Sciences.

Preparation of Maleimidobenzoyloxy Chitosan (*MB-chitosan*). MB-chitosan was prepared as previously described (*30*, *31*). Briefly, Chitosan (Chitosan-10, 80% deacetylated, molecular weight of 40000) was purchased from Wako Pure Chemical Industries, Ltd. (Osaka, Japan). Chitosan-10 (428 mg, 2.66 μmol of sugar unit) was dissolved in 2% AcOH (21 mL), and *N*-(*m*-maleimidobenzoyloxy)succinimide (MBS, 25 mg, 0.08 mmol) in 2 mL of DMF was added at 4 °C for 3 h. After addition of DMF (200 mL), the resulting precipitate was collected by centrifugation and washed with 75% methanol (twice) and with 100% methanol. The precipitated MB-chitosan was dissolved in 20% AcOH and freeze-dried (yield, 260 mg).

Antibodies. The rat monoclonal antibody against human integrin α6 (GoH3) was purchased from AMAC (Westbrook, ME). Mouse monoclonal antibodies against human integrins α1 (FB12), α2 (P1E6), α3 (P1B5), αv (P3G8), and β1 (6S6) were purchased from Millipore Co. Ltd. (Billerica, MA). Mouse monoclonal antibodies against human IgG heavy chain (MR36G) and vinculin (hVIN-1) were purchased from Sigma-Aldrich (St. Louis, MO).

Cells and Culture. HT1080 cells, a human fibrosarcoma cell line (HSRRB, Osaka, Japan), HaCaT cells, an immortalized aneuploid human keratinocyte cell line (*32*), and human neonatal dermal fibroblasts (HDFs) (IWAKI, Co. Ltd., Tokyo, Japan) were cultured in Dulbecco's modified Eagle's medium (DMEM, Invitrogen, Carlsbad, CA) containing 10% fetal bovine serum (FBS, Invitrogen), 100 units/mL penicillin, and 100 μg/mL streptomycin (Invitrogen). PC12 cells, a rat pheochromocytoma cell line (*32*), were cultured in DMEM containing 7.5% horse serum (Invitrogen), 7.5% FBS, 100 units/mL penicillin, and 100 μg/mL streptomycin. The cells were maintained at 37 °C in a humidified 5% CO_2/95% air atmosphere.

Cell Attachment Assay Using Peptide-Coated Plates. The cell attachment assay was performed in 96-well plates (Nunc, Roskilde, Denmark). Synthetic peptides were dissolved in Milli-Q water (1 mg/mL), and various amounts of the peptide solutions were added to each well and the wells dried overnight at room temperature. Then, the wells were blocked with 1% heat-denatured bovine serum albumin (BSA, Sigma) in DMEM at 37 °C for 1 h and then washed with 0.1% BSA in DMEM (twice). Cells were detached with 0.02% trypsin-EDTA (Invitrogen). The cells were allowed to recover in their respective culture medium for 20 min at 37 °C. After they were washed twice with 0.1% BSA in DMEM, cells were resuspended in 0.1% BSA in DMEM, plated at a density of 2.0×10^4 cells per 100 μL per well, and incubated at 37 °C for 1 h in 5% CO_2. The medium was removed by aspiration, and the attached cells were fixed and stained with a

[1]Abbreviations: ECM, extracellular matrix; DMF, *N*,*N*-dimethylformamide; HDFs, human dermal fibroblasts; DMEM, Dulbecco's modified Eagle's medium; FBS, fetal bovine serum; BSA, bovine serum albumin; EDTA, ethylenediaminetetraacetic acid; TBS, Tris-buffered saline; PBS, phosphate-buffered saline; DAPI, 4,6-diamidino-2-phenylindole.

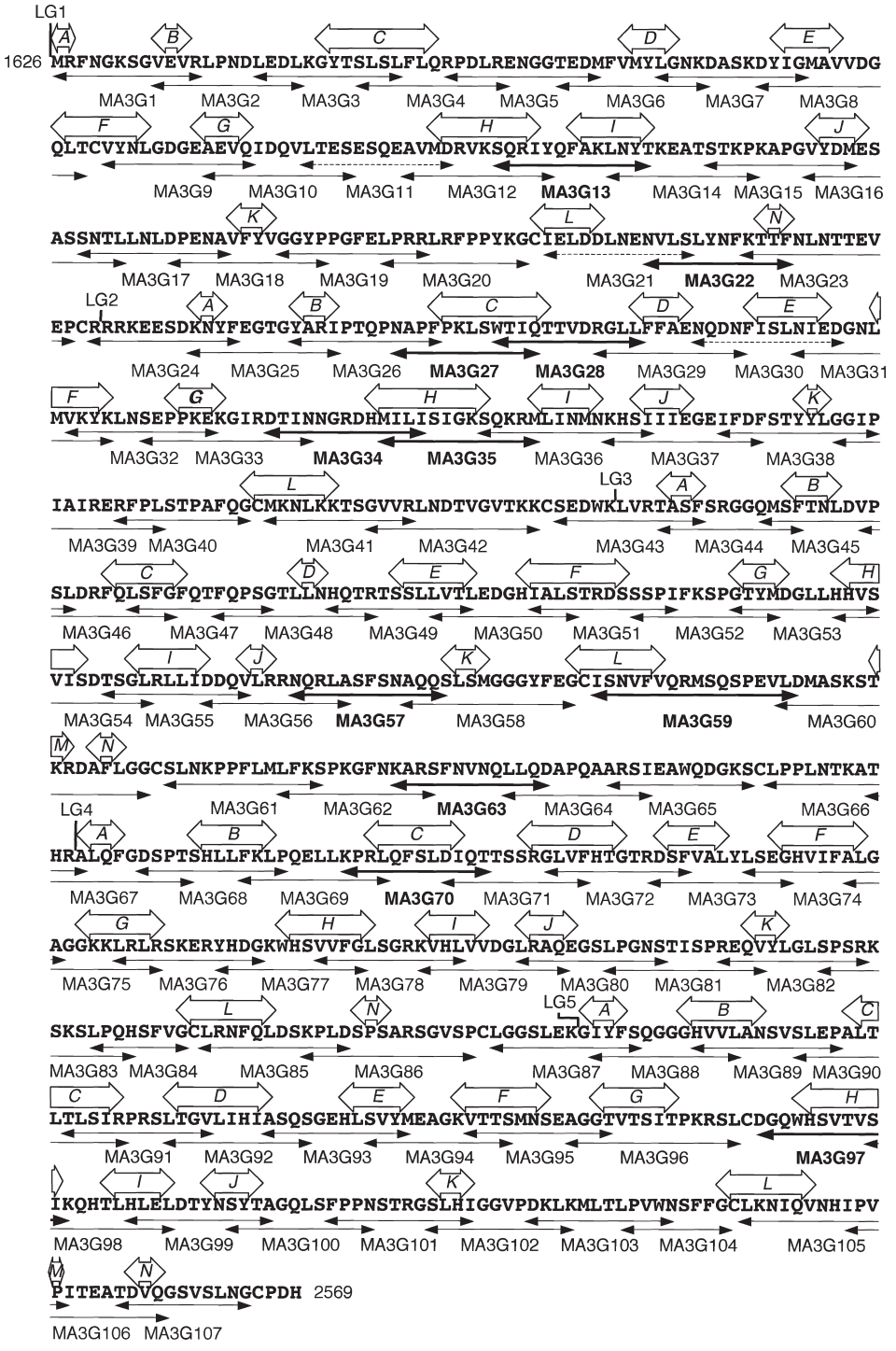

FIGURE 1: Sequence and peptides from the laminin α3 chain G domain. The sequence was derived from the mouse laminin α3 chain (positions 1626−2568) (*30*). Arrows denote the locations of peptides. Thick lines denote active peptides. Dashed lines denote insoluble peptides. Boxed arrows denote β strands.

0.2% crystal violet aqueous solution in 20% methanol for 15 min. After the wells were washed with Milli-Q water, a 1% sodium dodecyl sulfate (SDS) solution (150 μL) was added to each well to lyse the stained cells. The optical density at 570 nm was measured in a Safire plate reader (Tecan Austria GmbH, Grödig, Austria). All cell attachment assays were conducted in triplicate experiments.

Cell Attachment Assay Using Peptide-Conjugated Sepharose Beads. The synthetic peptides were coupled to cyanogen bromide (CNBr)-activated Sepharose 4B (GE Healthcare, London, U.K.) as described previously (*11*). CNBr-activated Sepharose was prewashed for 15 min with 1 mM HCl. The peptides (200 μg) were incubated with the CNBr-activated Sepharose (30 mg) in 1 mL of 0.1 M $NaHCO_3$ containing 0.5 M NaCl (pH 8.3) for 1 h at room temperature. The beads were washed with coupling buffer to remove the excess peptides, and then the remaining active groups on the beads were blocked with 1 M ethanolamine (pH 8.0) for 2 h. The peptide-conjugated beads were washed first with 0.1 M acetate buffer (pH 4.0) containing 0.5 M NaCl and then with 0.1 M Tris-HCl (pH 8.0) containing 0.5 M NaCl, and then the washings were repeated, resulting in at least three cycles of alternating pH. The resulting

peptide beads were stored in TBS. Prior to use for the cell attachment assay, the peptide beads were washed with Milli-Q water twice and then suspended in Milli-Q water.

The attachment of cells to the peptide beads was assessed in 96-well plates. The cells were detached as described above. The cells were resuspended in DMEM containing 0.1% BSA (1.0×10^5 cells per 100 μL per well) and incubated with a 3 mg/50 μL peptide bead solution for 1 h at 37 °C in 5% CO_2. The cells attached to the peptide beads were stained with a 0.2% crystal violet aqueous solution in 20% methanol for 15 min. After unattached cells had been removed and the wells had been washed with Milli-Q water, the attached cells were observed under a BZ-8000 microscope (Keyence, Osaka, Japan). Each experiment with different cell lines was examined in triplicate assays.

Cell Attachment Assay Using Peptide−Chitosan Membranes. Cell attachment assays using peptide−chitosan membranes were performed on 96-well plates (Nunc). The MB-chitosan was dissolved in 4% AcOH at 2 μg/mL, and 50 μL of the solution was added to each well on the 96-well plates. After drying at room temperature for 24 h, the plates were washed with 1% $NaHCO_3$ (100 μL) and then washed with PBS (100 μL, three times). For conjugation of peptides to chitosan membranes, a Cys-Gly-Gly (CGG) sequence was added at the N-terminus of the peptides. Cys-A99 (CGGAGTFALRGDNPQG) (*30*), Cys-A99T (CGGDGNLARAPGQFTG), Cys-MA3G57 (CGGNQ-RLASFSNAQQS), and Cys-MA3G57S (CGGSAQLSNFQA-RSQN) were synthesized as previously described (*30*, *31*). Peptide solutions (1 mg/mL) in 0.1% TFA Milli-Q water were prepared. Various amounts of peptide solutions diluted with 1% $NaHCO_3$ (50 μL/well) were added to the wells and incubated for 2 h. Then, the plates were washed with 1% BSA in DMEM three times, blocked by the addition of 1% BSA in DMEM for 30 min, and washed with 0.1% BSA in DMEM (three times). HDFs were detached as described above and were resuspended in DMEM containing 0.1% BSA. The cells were added (2.0×10^4 cells per 100 μL per well) to each well and incubated for 1 h at 37 °C in 5% CO_2. The cells attached to the peptide-conjugated chitosan membranes were stained with a 0.2% crystal violet aqueous solution in 20% methanol for 15 min. After unattached cells had been removed and the wells had been washed with Milli-Q water, the attached cells in three randomly selected fields were counted under a BZ-8000 microscope.

Inhibition Assay. For inhibition of the attachment of cells to peptide-coated plates, 96-well plates were coated with peptides as described above. The cells were preincubated for 15 min at 37 °C in the presence of either 10 μg/mL heparin, 5 mM ethylenediaminetetraacetic acid (EDTA), or 10 μg/mL anti-integrin antibodies prior to being plated in the wells. HDFs (2.0×10^4 cells per 100 μL per well) were incubated at 37 °C in 5% CO_2 for 30 min. After being stained with 0.2% crystal violet in 20% methanol for 15 min, the attached cells were counted under a BZ-8000 microscope.

For inhibition of the attachment of cells to the peptide−chitosan membranes, various amounts of peptides were conjugated to the chitosan membrane as described above. HDFs were incubated for 1 h at 37 °C on the peptide−chitosan membranes in the presence of either 10 μg/mL heparin or 5 mM EDTA. For inhibition of cell attachment with anti-integrin antibodies, HDFs were preincubated in suspension with 30 μg/mL anti-integrin antibodies for 15 min at 37 °C. Then HDFs (2.0×10^4 cells per 100 μL per well) were incubated on the peptide−chitosan plates for 1 h at 37 °C in 5% CO_2. After being stained with 0.2% crystal violet in 20% methanol for 15 min, the attached cells were counted under a BZ-8000 microscope. All assays were conducted in triplicate with each experiment repeated at least three times.

Immunocytochemistry. For immunostaining on the peptide-coated plates, eight-well glass chamber slides (Nunc) were coated with peptides (5 μg of MA3G27 and MA3G70 per well) and dried for 48 h. For immunostaining on the peptide-conjugated chitosan membranes, the chitosan membranes were prepared on eight-well Permanox Chamber Slides (Nunc) and dried for 48 h. After the plates had been washed with 1% $NaHCO_3$ and PBS, peptides (10 μg of MA3G57 per well) and 1% $NaHCO_3$ were added, and the mixture was incubated for 2 h. The wells were blocked with 1% BSA in DMEM for 1 h and washed with 0.1% BSA in DMEM (twice). Then, HDFs (8.0×10^3 cells per 200 μL per well) were added to the wells and incubated for 2 h at 37 °C in 5% CO_2. The cells were fixed with 4% paraformaldehyde and 5% sucrose in TBS for 10 min and permeabilized with 0.1% Triton X-100 in PBS for 10 min. The fixed cells were washed with PBS for 30 min, blocked with 1% BSA in PBS for 1 h, and then incubated with mouse monoclonal antibody against vinculin (clone hVIN-1; 1:100) overnight at 4 °C. After the samples had been washed twice with 0.05% Tween 20 in PBS for 15 min, bound antibody and actin filaments were labeled with a mixture of rhodamine red-labeled donkey anti-mouse IgG antibody (Jackson Immuno Research Laboratories, West Grove, PA) at 1:50 and Allexa Fluoro 488 phalloidin (1 unit/m; Invitrogen) at 1:100 for 2 h. Nuclei were labeled with 4,6-diamidino-2-phenylindole (DAPI, Invitrogen, 1:10000). After being washed with 0.05% Tween 20 in PBS for 10 min, the glass slides were desalted with Milli-Q water and mounted with a 50% glycerol solution containing anti fade. Images were captured with a Quantix CCD camera (Photometrics, München, Germany) and processed using IPLab (Scanalytics, Fairfax, VA). Deconvolution of the images was performed with HazeBuster (Vay Tek, Fairfield, IA).

Neurite Outgrowth Assay Using Peptide-Coated Plates. Neurite outgrowth was performed in 96-well plates coated with various amounts of peptides in 50 μL of Milli-Q water. Peptides were added to the wells and dried overnight at room temperature. The wells were washed twice with DMEM/F12 (Invitrogen) containing 30 nM Na_2SeO_3 (Wako). PC12 cells were primed with 100 ng/mL nerve growth factor (NGF, Invitrogen) for 24 h prior to the assay. The PC12 cells were then collected by agitation, allowed to recover in the cultured medium for 30 min at 37 °C in 5% CO_2, and washed twice with DMEM/F12. After being washed, cells were resuspended in DMEM/F12 containing 30 nM Na_2SeO_3, 100 μg/mL transferrin (Sigma), 20 nM progesterone (Sigma), 5 μg/mL insulin (Invitrogen), and 100 ng/mL NGF. The cells were added to 96-well plates at a density of 3.0×10^3 cells per 100 μL per well. After incubation at 37 °C for 24 h in 5% CO_2, the cells were fixed with 20% formalin and then stained with a 0.2% crystal violet aqueous solution in 20% methanol for 15 min. In each well, 100 cells were viewed under a BZ-8000 microscope, and the percent of active cells, which had neurites that extended twice a cell diameter in length and/or longer, was determined. Analyses of neurite outgrowth were conducted in triplicate.

RESULTS

Cell Attachment Activity on Peptide-Coated Plates. To identify biologically active sequences, we screened 104 soluble

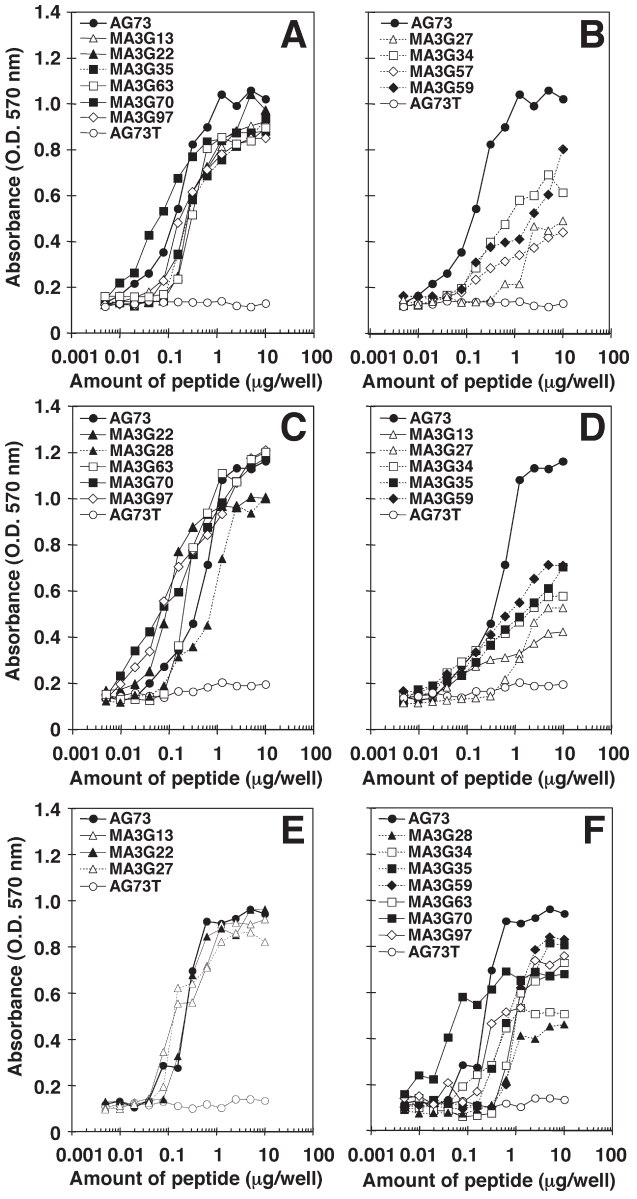

FIGURE 2: Attachment of cells to peptide-coated plates. Ninety-six-well plates were coated with various amounts of synthetic peptides and examined for cell attachment activity using HT1080 cells (A and B), HaCaT cells (C and D), and HDFs (E and F). The cells were added to the wells for 1 h. After the cells were stained with 0.2% crystal violet in 20% methanol, the attached cells were dissolved in 1% SDS, and the OD_{570} was measured. Data are expressed as means of triplicate results. Triplicate experiments gave similar results.

peptides covering the mouse laminin α3 chain C-terminal G domain (positions 1626−2569) (Figure 1). The peptides were coated on plates and examined for their cell attachment activity using HT1080 cells, HaCaT cells, and HDFs (Figure 2 and Table 1). The AG73 peptide (RKRLQVQLSIRT; mouse laminin α1 chain, residues 2719−2730), which has the strongest cell attachment activity in the α1 chain G domain, and its scrambled peptide AG73T (LQQRRSVLRTKI) were used as positive and negative controls, respectively (*11*).

First, we examined the cell attachment activity of the 104 soluble peptides on peptide-coated plates using HT1080 cells. Six peptides (MA3G13, MA3G22, MA3G35, MA3G63, MA3G70, and MA3G97) showed strong HT1080 cell attachment activity in a dose-dependent manner (Figure 2A). These cell attachment activities were comparable with that of AG73. Four peptides (MA3G27, MA3G34, MA3G57, and MA3G59) showed moderate cell attachment activity that was weaker than that of AG73 (Figure 2B). The remainder of the peptides did not promote HT1080 cell attachment.

We next evaluated cell attachment activity using HaCaT cells. Five peptides (MA3G22, MA3G28, MA3G63, MA3G70, and MA3G97) had strong HaCaT cell attachment activity comparable to that of AG73 (Figure 2C). Five peptides (MA3G13, MA3G27, MA3G34, MA3G35, and MA3G59) showed weak HaCaT cell attachment activity (Figure 2D). The remainder of the 93 soluble peptides did not promote HaCaT cell attachment.

Attachment of HDFs to the peptide-coated plates was also evaluated. HDFs strongly attached to three peptides coated on the plates (MA3G13, MA3G22, and MA3G27) with activity similar to that of AG73 (Figure 2E). Seven peptides (MA3G28, MA3G34, MA3G35, MA3G59, MA3G63, MA3G70, and MA3G97) exhibited weak HDF attachment activity (Figure 2F). None of the other peptides exhibited HDF attachment. Further, HDFs on MA3G27 were well spread, while on MA3G28, weaker spreading was observed. The other active peptides did not have cell spreading activity (Table 1).

Cell Attachment Activity on Peptide-Conjugated Sepharose Beads. Next, we conjugated the 104 soluble peptides with CNBr-activated Sepharose beads and tested their cell attachment activity using HT1080 cells, HaCaT cells, and HDFs (Table 1). AG73- and AG73T-conjugated Sepharose beads were used as positive and negative controls, respectively (*11*). HT1080 cells attached to six peptide-conjugated beads (MA3G13, MA3G27, MA3G35, MA3G57, MA3G70, and MA3G97) (Figure 3). None of the remaining peptide beads promoted HT1080 cell attachment. We also evaluated the cell attachment activity of peptide-conjugated beads using HaCaT cells and HDFs (data not shown). Both cells attached to the same six peptide beads in a manner similar to that observed with HT1080 cells (Table 1).

Neurite Outgrowth Activity of the Mouse Laminin α3 Chain G Domain Peptides. The 104 soluble peptides were evaluated for neurite outgrowth activity using PC12 cells, a rat pheochromocytoma cell line (Figure 4). AG73 and AG73T were used as positive and negative controls, respectively (*33*). Four peptides (MA3G27, MA3G35, MA3G57, and MA3G70) promoted neurite outgrowth activity in a dose-dependent manner (Figure 4A,B). These four peptides also exhibited cell attachment activity (Table 1). In contrast, the remaining peptides did not exhibit neurite outgrowth activity. These results suggest that the four active sequences have a potential to interact with neuronal cells in the laminin α3 chain G domain. On the basis of the two cell attachment assays using three different cells and the neurite outgrowth assay, we identified 11 biologically active peptides (Table 1).

Effects of Heparin and EDTA on Attachment of HDFs to Peptide-Coated Plates. To identify the cellular ligands, we next examined the effects of heparin and EDTA on attachment of HDFs to the 10 active peptides that were coated onto plates (Figure 5). AG73, which interacts with syndecans and promotes heparin-dependent cell adhesion (*11*), and EF-1 (DYATLQLQEGRLHFMFDLG; mouse laminin α1 chain, residues 2747−2765), which interacts with α2β1 integrin and promotes divalent cation-dependent cell adhesion (*27*), were used as controls. Attachment of HDFs to AG73 was inhibited by only heparin, and that to EF-1 was inhibited by only EDTA as shown previously (*11*, *27*) (Figure 5). Attachment of HDFs to eight of

Table 1: Synthetic Peptides and Their Biological Activities

		cell attachment							
		HT1080		HaCaT		HDFs			
peptide	sequence	plate[a]	bead[b]	plate	bead	plate	bead	cell attachment inhibition[c]	neurite outgrowth[d] (PC12)
MA3G13	SQRIYQFAKLNYT	++	+	+	+	++	+	heparin	−
MA3G22	NVLSLYNFKTTF	++	−	++	−	++	−	heparin	−
MA3G27	NAPFPKLSWTIQ	+	+	+	+	++S[e]	+	EDTA	+
MA3G28	WTIQTTVDRGLL	−	−	++	−	+s[e]	−	EDTA	−
MA3G34	DTINNGRDHMILI	+	−	+	−	+	−	heparin	−
MA3G35	MILISIGKSQKRM	++	+	+	+	+	+	heparin	+
MA3G57	NQRLASFSNAQQS	+	+	−	+	+	+	EDTA[f]	+
MA3G59	ISNVFVQRMSQSPEVLD	+	−	+	−	+	−	heparin	−
MA3G63	KARSFNVNQLLQD	++	−	++	−	+	−	heparin	−
MA3G70	KPRLQFSLDIQT	++	+	++	+	+	+	heparin	+
MA3G97	DGQWHSVTVSIK	++	+	++	+	+	+	heparin	−
AG73	RKRLQVQLSIRT	++	+	++	+	++	+	heparin	+
AG73T	LQQRRSVLRTKI	−	−	−	−	−	−		−

[a]For cell attachment assays on plates, various amounts of the peptides were coated on 96-well plates as described in Materials and Methods. HT1080 human fibrosarcoma cells, HaCaT human skin keratinocyte cells, and human neonatal dermal fibroblasts (HDFs) were used. The peptide-coated plate assays were quantitated and assessed relative to those observed with AG73 and evaluated on the following subjective scale: ++, attachment comparable to that on AG73; +, weak attachment compared with that on AG73; −, no adhesion. [b]For cell attachment assays on beads, the peptides were coupled to CNBr-activated Sepharose 4B as described in Materials and Methods. HT1080 cells, HaCaT cells, and HDFs were used. The peptide-conjugated bead assays were evaluated on the following subjective scale: +, promotes cell attachment; −, no promotion. [c]EDTA and heparin inhibited attachment of HDFs to the peptide-coated plates or the peptide−chitosan membrane. Inhibited compounds (EDTA or heparin) are shown. [d]Neurite outgrowth of PC12 rat pheochromocytoma cells was evaluated on the following subjective scale: +, promotes neurite outgrowth; −, no promotion. [e]S and s mean extensive and weak cell spreading, respectively. [f]The compound that inhibited attachment of cells to the MA3G57−chitosan membrane is shown.

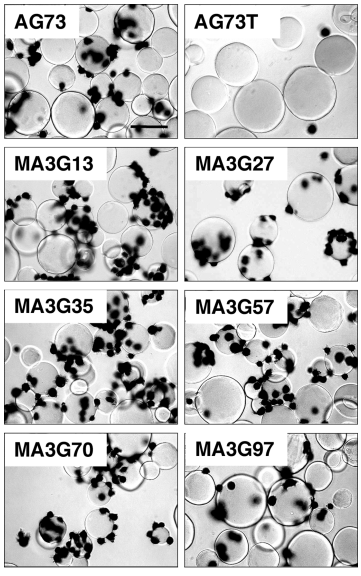

FIGURE 3: Attachment of cells to peptide-conjugated Sepharose beads. HT1080 cells were allowed to attach to peptide−Sepharose beads for 1 h and were then stained with 0.2% crystal violet in 20% methanol. Triplicate experiments gave similar results. The bar is 100 μm.

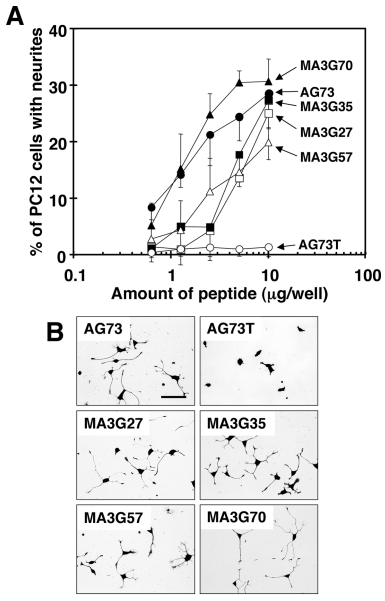

FIGURE 4: Neurite outgrowth of PC12 cells on synthetic peptides. (A) Various amounts of peptides were coated on 96-well plates. PC12 cells (3.0 × 103 cells/well) were seeded in the wells and incubated for 24 h. After the cells were fixed and stained, the percentage of cells with neurites was determined as described in Materials and Methods. Data are expressed as means ± the standard deviation of triplicate mesurements. Triplicate experiments gave similar results. (B) Photographs of the PC12 cells incubated on 10 μg of peptide/well. After a 24 h incubation, the cells were fixed and stained and then photographed with a 200× objective on a microscope. The bar is 100 μm.

the peptides was significantly inhibited by heparin, with attachment to MA3G27 and MA3G28 not blocked by heparin. In contrast, attachment of HDFs to MA3G27 and MA3G28 was significantly inhibited by EDTA. Attachment of HDFs to MA3G59 was slightly inhibited by EDTA, but the inhibition was not statistically significant. Attachment of HDFs to the remaining peptides was not affected by EDTA (Figure 5). HDFs attached to MA3G27 and MA3G28 in a divalent cation-dependent fashion, suggesting that the cellular interaction with these peptides involves integrins. In contrast, attachment of HDFs to eight peptides was heparin-dependent, indicating that these eight peptides may bind to membrane-associated HSPGs, including syndecans.

Organization of Actin Filaments and Localization of Vinculin in HDFs on Synthetic Peptides. The results in the

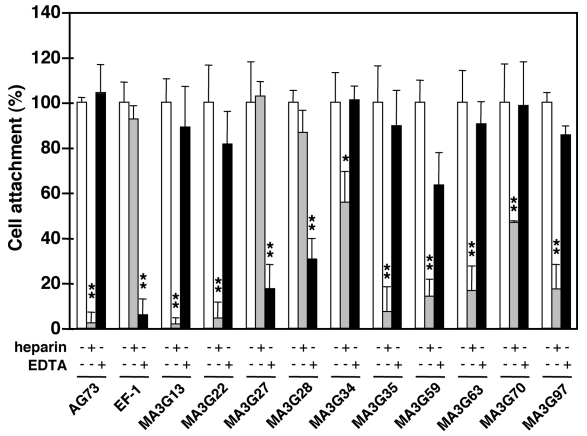

FIGURE 5: Effect of heparin and EDTA on the attachment of HDFs to peptides. HDFs were allowed to attach to the peptide-coated plates in the absence (white bars) and presence of either 10 μg/mL heparin (gray bars) or 5 mM EDTA (black bars). Ninety-six-well plates were coated with 0.5 μg/well (AG73 and EF-1), 2.5 μg/well (MA3G13, MA3G22, MA3G27, MA3G70, and MA3G97), or 5 μg/well (MA3G28, MA3G34, MA3G35, MA3G54, and MA3G59). Either 10 μg/mL heparin or 5 mM EDTA was added to the cells, and then the cells were added to the plates. After a 30 min incubation, the attached cells were stained with 0.2% crystal violet in 20% methanol and the adherent cells were counted under a microscope. Each value represents the mean of three separate determinations ± the standard deviation. Triplicate experiments gave similar results. *$p < 0.01$; **$p < 0.001$.

inhibition and cell attachment assays suggested that MA3G27 has extensive cell spreading activity and that this adhesion to MA3G27 is mediated by integrin. In contrast, MA3G70, a homologous α3 chain sequence of AG73 (*34*), exhibited heparin-dependent cell attachment and neurite outgrowth activity similar to that of AG73. Integrins connect to intracellular proteins and modulate cell morphology. Therefore, we evaluated the organization of the cytoskeleton and the localization of vinculin in HDFs attached to the active peptides by immunostaining (Figure 6). MA3G27 induced well-organized actin stress fibers and focal contacts containing vinculin (Figure 6A). In contrast, HDFs on MA3G70 showed accumulation of actin at the edges of cells with spikelike ruffling membranes, but focal adhesions were not observed (Figure 6B). These results demonstrate that the active peptides affect the organization of the cytoskeleton in HDFs and are biologically active in a peptide-specific manner.

Effect of Anti-Integrin Antibodies on Attachment of HDFs to MA3G27. Since the attachment of HDFs to MA3G27 was divalent cation-dependent, it is possible that integrins are major candidates for the cellular receptor(s). We attempted to identify the cell surface receptors for MA3G27 using function-blocking antibodies against integrin subunits (Figure 7). We examined the effect of anti-integrin subunit antibodies on the attachment of HDFs to this peptide. Attachment of HDFs to MA3G27 was significantly inhibited by both anti-α6 and anti-β1 integrin antibodies. In contrast, the other integrin antibodies, anti-α1, -α2, -α3, and -αv, did not affect the attachment of HDFs to MA3G27. These results suggest that the attachment of HDFs to MA3G27 is mediated by α6β1 integrin.

Biological Activities on Peptide−Chitosan Membranes. On the plates, MA3G57 showed poor cell attachment activity with only HT1080 cells. However, on the beads, MA3G57 exhibited the activity with all three cell lines (Table 1). Next, we conjugated MA3G57 to chitosan membranes and further

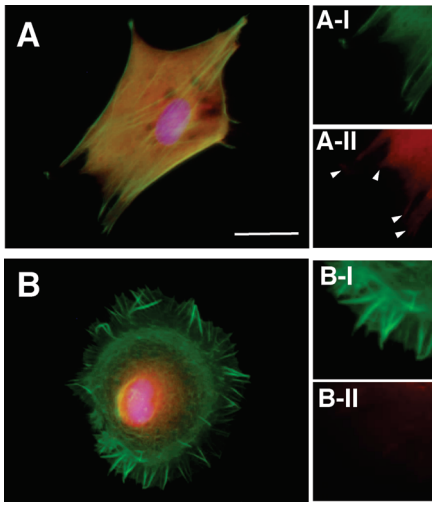

FIGURE 6: Organization of actin stress fibers and localization of vinculin. Eight-well chamber slides were coated with 5 μg of MA3G27 (A) or MA3G70 (B) per well. HDFs were seeded as described in Materials and Methods. After a 2 h incubation, attached cells were fixed with 4% paraformaldehyde. Triple-color fluorescence microscopy was preformed for simultaneous detection of actin filaments (green), vinculin (red), and nuclei (blue). The localization of vinculin was assessed with a mouse monoclonal antibody against vinculin, followed by detection with a rhodamine red-labeled donkey anti-mouse IgG antibody. Actin filaments and nuclei were visualized by incubation with Allexa Fluoro 488 phalloidin and DAPI, respectively. Merged images are shown in panels A and B. Localization of actin (A-I and B-I) and vinculin (A-II and B-II) is also shown in separate images. The arrows indicate the vinculin staining in focal contacts. The bar is 50 μm.

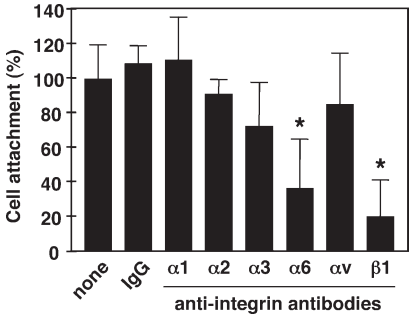

FIGURE 7: Effect of anti-integrin subunit antibodies on the attachment of HDFs to MA3G27. Ninety-six-well plates were coated with MA3G27 (1.5 μg/well). HDFs in a cell suspension were preincubated with 10 μg/mL integrin antibodies at room temperature for 15 min, then added to the wells, and incubated for 30 min. Following staining with 0.2% crystal violet in 20% methanol, the number of attached cells was counted. Each value represents the mean of three separate determinations ± the standard deviation. Duplicate experiments gave similar results. *$p < 0.01$.

tested the biological activities using the peptide−chitosan membranes (Figure 8). From the laminin α1 chain screening, A99 (AGTFALRGDNPQG; mouse laminin α1 chain, residues 1141−1153) containing an Arg-Gly-Asp (RGD) sequence was identified as a cell attachment-promoting peptide only in the bead assay (*6*). Recently, we found that A99 promotes α$v\beta$3 integrin-mediated cell attachment when the peptide is conjugated on a chitosan membrane (*30*, *31*). Cys peptides were prepared and conjugated on MB-chitosan membranes as described in Materials and Methods. Cys-A99 and Cys-A99T were used as positive and negative controls, respectively.

HDF attachment was evaluated on the MA3G57−chitosan membranes. Attachment was promoted on the A99−chitosan

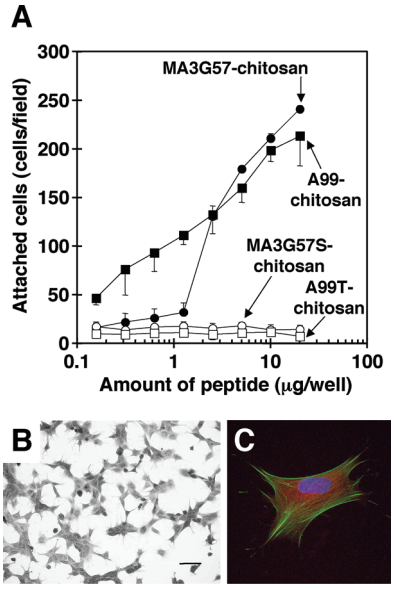

FIGURE 8: Cell attachment activity of MA3G57 peptide−chitosan membranes. (A) HDF attachment activity of peptide−chitosan membranes. Various amounts of peptides were coupled to the chitosan membranes as described in Materials and Methods. HDFs were incubated on the peptide−chitosan membranes for 1 h. After the cells were stained with 0.2% crystal violet in 20% methanol, the number of attached cells was counted under a microscope. Each value represents the mean of three separate determinations ± the standard deviation. Triplicate experiments gave similar results. (B) Morphological appearance of HDFs on the MA3G57−chitosan membrane. The wells were coated with 10 μg of MA3G57−chitosan membrane per well. HDFs were added to the wells as described in Materials and Methods. After a 2 h incubation, attached cells were stained with crystal violet. Triplicate experiments gave similar results. The bar is 100 μm. (C) Organization of actin filaments and localization of vinculin in HDFs on MA3G57−chitosan membranes. Eight-well chamber slides were coated with 10 μg of MA3G57−chitosan membranes per well. Cells were seeded as described in Materials and Methods. After a 2 h incubation, attached cells were fixed with 4% paraformaldehyde. Triple-color fluorescence microscopy was preformed for simultaneous detection of actin filaments (green), vinculin (red), and nuclei (blue). Merged images are shown in panel C.

membrane in a dose-dependent manner but not on the A99T−chitosan membrane as expected (Figure 8A). The MA3G57−chitosan membrane showed HDF attachment activity similar to that observed on the A99−chitosan membrane. In contrast, a scrambled MA3G57 peptide, MA3G57S-conjugated chitosan membrane did not show activity. These results indicate that the MA3G57 peptide is active for cell attachment on the chitosan membrane. HDFs on the MA3G57−chitosan membrane (10 μg/well) were well-spread (Figure 8B). We next observed the organization of the cytoskeleton and the localization of vinculin in HDFs attached to the MA3G57−chitosan membrane (Figure 8C). The MA3G57−chitosan membrane promoted typical fibroblast type morphology, and well-developed focal contacts containing vinculin with filopodia were observed (Figure 8C). These data suggest that the MA3G57−chitosan membrane induces a peptide-specific cellular response.

To clarify the mechanism of adhesion of cells to the MA3G57−chitosan membrane, we examined the inhibitory effect of heparin and EDTA on the attachment of cells to the MA3G57−chitosan membrane (Figure 9). Attachment of cells to the MA3G57−chitosan membrane was significantly inhibited by EDTA but not by heparin, suggesting that this MA3G57 peptide

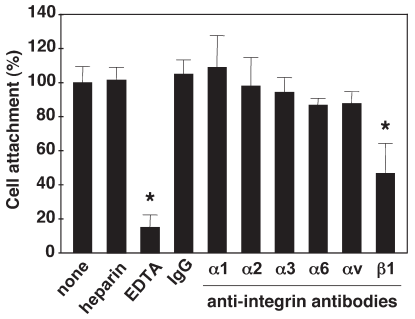

FIGURE 9: Effect of heparin, EDTA, and anti-integrin subunit antibodies on the attachment of HDFs to MA3G57−chitosan membranes. Ninety-six-well plates were coated with 5 μg of MA3G57−chitosan membrane per well. Either 10 μg/mL heparin, 5 mM EDTA, or 30 μg/mL anti-integrin antibodies were added to the cell suspensions. The cell suspensions in the presence of 30 μg/mL anti-integrin antibodies were preincubated at room temperature for 15 min. Then the cells were added to the wells and incubated for 1 h. After being stained with crystal violet, the attached cells were counted under a microscope. Each value represents the mean of three separate determinations ± the standard deviation. Duplicate experiments gave similar results. *$p < 0.001$.

promotes divalent cation-dependent cell adhesion. We also evaluated the effect of anti-integrin antibodies on the attachment of HDFs to the MA3G57−chitosan membrane (Figure 9). Attachment of cells to the MA3G57−chitosan membrane was partially blocked by the anti-β1 integrin antibody. In contrast, none of the other anti-integrin antibodies inhibited the attachment of cells to the MA3G57−chitosan membrane. These results suggest that the MA3G57−chitosan membrane is involved in β1 integrin-mediated cell attachment and spreading.

DISCUSSION

The laminin α3 chain is strongly expressed in skin, lung, olfactory epithelium, and the superficial layers of the tongue and palate. The G domain at its carboxyl terminus interacts with various ECM molecules and receptors (*35*). Biologically active sites in the human laminin α3 chain have been well characterized. Recently, it has been shown that the human laminin α3 chain LG1-3 module promotes cell adhesion and spreading via integrins, and the P4 peptide (PPFLMLLKGSTR; human laminin α3 chain, residues 1312−1323) in the α3 chain LG3 module is crucial for binding of α3β1 integrin to human normal keratinocyte and stimulates focal adhesion kinase (FAK) phosphorylation (*36*). We found that the corresponding mouse sequence of the P4 peptide, the overlapping region between MA3G61 and MA3G62, did not exhibit any activity. The low degree of homology between human and murine laminin α3 chains suggests that the P4 peptide region is a human-specific active sequence. On the other hand, the human laminin α3 chain LG4 module interacts with syndecans on keratinocytes (*24*, *25*, *37*). The A3G756 peptide, which is located on the E and F strands connecting the loop region in the human laminin α3 chain LG4 module, is a critical sequence for the biological activities of the LG4 module (*22*−*25*, *28*). Further, the loop structure of the E−F strand connecting region of A3G756 within the human laminin α3 chain LG4 module is important for biological activity (*28*). Mouse A3G756 (formerly termed EF-3, RDSFVALYLSEGHVIFALG; mouse laminin α3 chain, residues 2266−2284) did not exhibit cell attachment activity but promoted neurite outgrowth (*27*). MA3G73 and MA3G74 covering the mouse A3G756 sequence did not exhibit any biological activity.

Previous studies with recombinant protein also demonstrated that the human and mouse laminin α3 chain G domains undergo different proteolytic degradation (*38*). The sequence of the mouse laminin α3 chain G domain is 86% homologous with the human sequence. The α3 chain G domain may have some species-specific activities.

In this study, we have used peptide-coated plate and peptide-conjugated Sepharose bead assays. MA3G13, MA3G27, MA3G35, MA3G70, and MA3G97 exhibited cell attachment activity in both plate and bead assays. On the other hand, MA3G22, MA3G28, MA3G34, MA3G57, MA3G59, and MA3G63 were active in either the plate or bead assays. These results strongly support the possibility that both methods should be employed when testing for cell attachment activity of peptides. It is likely that the differential activities are due to inactive conformations and/or poor coating efficiencies on the plate. For example, five peptides, MA3G22, MA3G28, MA3G34, MA3G59, and MA3G63, exhibited cell attachment activity in the plate assay, whereas these peptides were inactive in the bead assay. We have previously reported that the 12-mer peptide containing the IKVAV sequence from the laminin α1 chain (*39*) was active in the peptide-coated plate assay but was not active in the peptide-conjugated bead assay (*6*). More recently, it has been reported that LAM-L, an IKVAV peptide derived from the laminin α1 chain, forms β sheet structures, such as amyloid-like fibrils, and promotes cell adhesion and neurite outgrowth (*40*). Taken together, it is important to employ two different assays in identifying biologically active sites when performing a systematic peptide screening.

Integrins are major cell surface receptors involved in cell adhesion, migration, proliferation, and survival. The LG1-3 module of the laminin α3 chain binds to α3β1, α6β1, and α6β4 integrins (*15*). Previously, we found the EF-1 peptide was an α2β1 integrin binding site in the laminin α1 chain LG4 module (*27*). Attachment of HDFs to EF-1 was significantly blocked by anti-α2 and anti-β1 integrin antibodies, and EF-1 inhibited the cell attachment activity of recombinant α1LG4-5 (*27*). Our site-directed mutagenesis of the laminin α1 chain LG4 module demonstrated that the EF-1 site is crucial for cell spreading activity via α2β1 integrin (*41*). The MA3G27 peptide exhibited divalent cation-dependent cell adhesion and spreading activities, and attachment of HDFs to MA3G27 was significantly inhibited by anti-α6 and β1 integrin antibodies. We also observed well-organized actin stress fibers and vinculin accumulation in focal contacts in HDFs on MA3G27. These results suggest that the MA3G27 sequence promotes α6β1 integrin-mediated cell adhesion. More recently, the crystal structure of the laminin α2 chain LG1-3 module was determined (*42*), and the MA3G27 sequence is located on the C strand of the LG2 module. The recombinant human laminin α3 chain LG2 module has divalent cation-dependent cell attachment activity and recognizes not only α3β1 but also α6β1 integrins (*19*). Therefore, we also evaluated the cell attachment activity of the HA3G27 peptide (HAPIPTFGQTIQ; human laminin α3 chain, residues 996−1007), a corresponding human sequence of MA3G27. While MA3G27 exhibited strong cell attachment activity, HA3G27 did not promote cell attachment in any of the cell lines (data not shown). These results suggest that the MA3G27 sequence is a specific active site in mouse for the interaction between the laminin α3 chain LG2 module and α6β1 integrin.

The laminin α3 chain binds not only to integrins but also to HSPGs (*19*, *22*, *37*). Previously, we identified AG73 (*11*, *34*), A3G756 (*22*, *24*), and A4G20 (DVISLYNFKHIY; mouse laminin α4 chain, residues 1008−1019) (*43*) as syndecan-binding sites in the laminin α chain G domain. AG73 interacts with syndecan-1 through heparin/heparan sulfate side chains (*34*), and the adhesion of HDFs to AG73 specifically induced actin filament spikes associated with membrane ruffling (*41*). MA3G70, a homologous sequence of AG73, exhibited strong cell attachment activity and promoted actin filament spikes similar to those generated by AG73. These results suggest that MA3G70 promotes syndecan-mediated cell attachment comparable to that of AG73.

MA3G28 exhibited strong cell attachment activity with HaCaT cells. The activity was inhibited by EDTA (data not shown). These results suggest that MA3G28 in a divalent cation-dependent manner interacts with specific cellular receptors on HaCaT cells, such as integrins. Since the loss of β1 integrin in vivo in keratinocytes caused a severe defect in wound healing (*44*), we suggest that MA3G28 could be useful for the development of therapeutic reagents for wound healing and tissue regeneration. The MA3G28 sequence is located on the loop region between the C and D strands in the laminin α3 chain LG2 module. The crystal structure showed that the MA3G28 sequence is structurally important for stabilizing the LG2-3 site (*42*). Additionally, MA3G28 neighbors the MA3G27 sequence overlapping four C-terminal amino acids (WTIQ) of MA3G28. These considerations predict that the MA3G27 and MA3G28 sequences may synergistically contribute to integrin interactions, but this needs to be tested further.

MA3G57 exhibited weak cell attachment activity on the plates with only HT1080 cells and exhibited attachment activity on the beads with all three cell lines. We therefore prepared MA3G57-conjugated chitosan membranes and tested their biological activity. The MA3G57−chitosan membrane exhibited a dose-dependent HDF attachment activity. EDTA and a functional blocking antibody against β1 integrin inhibited the attachment of cells to the MA3G57−chitosan membranes, suggesting that adhesion of cells to the MA3G57 sequence depends on divalent cations and is mediated by β1 integrin. MA3G57 is located in the connecting region between the J and K strands in the LG3 module. The loop structure of MA3G57 may be important for the biological activity. We conclude that cell adhesion assays using peptide-conjugated beads and chitosan membranes are useful for assessing the conformation-dependent biological functions.

We identified 11 biologically active sequences from the laminin α3 chain G domain using three different cell lines. Interestingly, all the active sequences newly identified in this study had basic amino acid residues (Lys or Arg) as a common feature. These results suggest that the basic amino acids contribute to the binding to cellular receptor(s). Nine of 11 identified active sequences were located in the LG1-3 module of the laminin α3 chain. These results suggest that the nine active sequences are major biologically active sites in the LG1-3 module. Additionally, MA3G27, MA3G28, and MA3G57 from the LG1-3 module specifically interacted with cells through integrins. Since the laminin α3 chain LG1-3 module also interacts with some integrins, these three active peptides may have potential to be the integrin-binding sites in the laminin α3 chain LG1-3 module. On the other hand, two peptides, MA3G70 and MA3G97, were identified as the active sequences from the LG4-5 module. We found through inhibition studies that the attachment of cells to MA3G70 and MA3G97 is dependent on heparin and/or HSPGs.

The LG4-5 module is proteolytically removed from the laminin α3 chain and interacts with HSPGs. Thus, we predict that MA3G70 and MA3G97 of the laminin α3 chain LG4-5 module play a prominent role in the binding to heparin and/or HSPGs. These peptides could be involved in the biological activities related to the laminin α3 chain G domain and would be useful for studying the molecular mechanisms of laminin receptor-mediated interactions. Our findings here may provide new insights for the molecular dissection of the C-terminal globular domain of the mouse laminin α3 chain and possibly also identify cryptic sites.

REFERENCES

1. Colognato, H., and Yurchenco, P. D. (2000) Form and function: The laminin family of heterotrimers. *Dev. Dyn. 218*, 213–234.
2. Miner, J. H., and Yurchenco, P. D. (2004) Laminin functions in tissue morphogenesis. *Annu. Rev. Cell Dev. Biol. 20*, 255–284.
3. Aumailley, M., Bruckner-Tuderman, L., Carter, W. G., Deutzmann, R., Edgar, D., Ekblom, P., Engel, J., Engvall, E., Hohenester, E., Jones, J. C., Kleinman, H. K., Marinkovich, M. P., Martin, G. R., Mayer, U., Meneguzzi, G., Miner, J. H., Miyazaki, K., Patarroyo, M., Paulsson, M., Quaranta, V., Sanes, J. R., Sasaki, T., Sekiguchi, K., Sorokin, L. M., Talts, J. F., Tryggvason, K., Uitto, J., Virtanen, I., von der Mark, K., Wewer, U. M., Yamada, Y., and Yurchenco, P. D. (2005) A simplified laminin nomenclature. *Matrix Biol. 24*, 326–332.
4. Yan, H. H., and Cheng, C. Y. (2006) Laminin α3 forms a complex with β3 and γ3 chains that serves as the ligand for α6β1-integrin at the apical ectoplasmic specialization in adult rat testes. *J. Biol. Chem. 281*, 17286–17303.
5. Nomizu, M., Kim, W. H., Yamamura, K., Utani, A., Song, S. Y., Otaka, A., Roller, P. P., Kleinman, H. K., and Yamada, Y. (1995) Identification of cell binding sites in the laminin α1 chain carboxyl-terminal globular domain by systematic screening of synthetic peptides. *J. Biol. Chem. 270*, 20583–20590.
6. Nomizu, M., Kuratomi, Y., Malinda, K. M., Song, S. Y., Miyoshi, K., Otaka, A., Powell, S. K., Hoffman, M. P., Kleinman, H. K., and Yamada, Y. (1998) Cell binding sequences in mouse laminin α1 chain. *J. Biol. Chem. 273*, 32491–32499.
7. Nomizu, M., Kuratomi, Y., Ponce, M. L., Song, S. Y., Miyoshi, K., Otaka, A., Powell, S. K., Hoffman, M. P., Kleinman, H. K., and Yamada, Y. (2000) Cell adhesive sequences in mouse laminin β1 chain. *Arch. Biochem. Biophys. 378*, 311–320.
8. Nomizu, M., Kuratomi, Y., Song, S. Y., Ponce, M. L., Hoffman, M. P., Powell, S. K., Miyoshi, K., Otaka, A., Kleinman, H. K., and Yamada, Y. (1997) Identification of cell binding sequences in mouse laminin γ1 chain by systematic peptide screening. *J. Biol. Chem. 272*, 32198–32205.
9. Yamada, K. M. (1991) Adhesive recognition sequences. *J. Biol. Chem. 266*, 12809–12812.
10. Yamada, Y., and Kleinman, H. K. (1992) Functional domains of cell adhesion molecules. *Curr. Opin. Cell Biol. 4*, 819–823.
11. Suzuki, N., Ichikawa, N., Kasai, S., Yamada, M., Nishi, N., Morioka, H., Yamashita, H., Kitagawa, Y., Utani, A., Hoffman, M. P., and Nomizu, M. (2003) Syndecan binding sites in the laminin α1 chain G domain. *Biochemistry 42*, 12625–12633.
12. Suzuki, N., Yokoyama, F., and Nomizu, M. (2005) Functional sites in the laminin α chains. *Connect. Tissue Res. 46*, 142–152.
13. Timpl, R., Tisi, D., Talts, J. F., Andac, Z., Sasaki, T., and Hohenester, E. (2000) Structure and function of laminin LG modules. *Matrix Biol. 19*, 309–317.
14. Nguyen, B. P., Gil, S. G., and Carter, W. G. (2000) Deposition of laminin 5 by keratinocytes regulates integrin adhesion and signaling. *J. Biol. Chem. 275*, 31896–31907.
15. Sugawara, K., Tsuruta, D., Ishii, M., Jones, J. C., and Kobayashi, H. (2008) Laminin-332 and -511 in skin. *Exp. Dermatol. 17*, 473–480.
16. Marinkovich, M. P., Lunstrum, G. P., Keene, D. R., and Burgeson, R. E. (1992) The dermal-epidermal junction of human skin contains a novel laminin variant. *J. Cell Biol. 119*, 695–703.
17. Tsubota, Y., Yasuda, C., Kariya, Y., Ogawa, T., Hirosaki, T., Mizushima, H., and Miyazaki, K. (2005) Regulation of biological activity and matrix assembly of laminin-5 by COOH-terminal, LG4-5 domain of α3 chain. *J. Biol. Chem. 280*, 14370–14377.
18. Kariya, Y., Tsubota, Y., Hirosaki, T., Mizushima, H., Puzon-McLaughlin, W., Takada, Y., and Miyazaki, K. (2003) Differential regulation of cellular adhesion and migration by recombinant laminin-5 forms with partial deletion or mutation within the G3 domain of α3 chain. *J. Cell. Biochem. 88*, 506–520.
19. Mizushima, H., Takamura, H., Miyagi, Y., Kikkawa, Y., Yamanaka, N., Yasumitsu, H., Misugi, K., and Miyazaki, K. (1997) Identification of integrin-dependent and -independent cell adhesion domains in COOH-terminal globular region of laminin-5 α3 chain. *Cell Growth Differ. 8*, 979–987.
20. Shang, M., Koshikawa, N., Schenk, S., and Quaranta, V. (2001) The LG3 module of laminin-5 harbors a binding site for integrin α3β1 that promotes cell adhesion, spreading, and migration. *J. Biol. Chem. 276*, 33045–33053.
21. Ryan, M. C., Lee, K., Miyashita, Y., and Carter, W. G. (1999) Targeted disruption of the LAMA3 gene in mice reveals abnormalities in survival and late stage differentiation of epithelial cells. *J. Cell Biol. 145*, 1309–1323.
22. Utani, A., Nomizu, M., Matsuura, H., Kato, K., Kobayashi, T., Takeda, U., Aota, S., Nielsen, P. K., and Shinkai, H. (2001) A unique sequence of the laminin α3 G domain binds to heparin and promotes cell adhesion through syndecan-2 and -4. *J. Biol. Chem. 276*, 28779–28788.
23. Kato, K., Utani, A., Suzuki, N., Mochizuki, M., Yamada, M., Nishi, N., Matsuura, H., Shinkai, H., and Nomizu, M. (2002) Identification of neurite outgrowth promoting sites on the laminin α3 chain G domain. *Biochemistry 41*, 10747–10753.
24. Araki, E., Momota, Y., Togo, T., Tanioka, M., Hozumi, K., Nomizu, M., Miyachi, Y., and Utani, A. (2009) Clustering of syndecan-4 and integrin β1 by laminin α3 chain-derived peptide promotes keratinocyte migration. *Mol. Biol. Cell 20*, 3012–3024.
25. Utani, A., Momota, Y., Endo, H., Kasuya, Y., Beck, K., Suzuki, N., Nomizu, M., and Shinkai, H. (2003) Laminin α3 LG4 module induces matrix metalloproteinase-1 through mitogen-activated protein kinase signaling. *J. Biol. Chem. 278*, 34483–34490.
26. Hohenester, E., Tisi, D., Talts, J. F., and Timpl, R. (1999) The crystal structure of a laminin G-like module reveals the molecular basis of α-dystroglycan binding to laminins, perlecan, and agrin. *Mol. Cell 4*, 783–792.
27. Suzuki, N., Nakatsuka, H., Mochizuki, M., Nishi, N., Kadoya, Y., Utani, A., Oishi, S., Fujii, N., Kleinman, H. K., and Nomizu, M. (2003) Biological activities of homologous loop regions in the laminin α chain G domains. *J. Biol. Chem. 278*, 45697–45705.
28. Kato-Takagaki, K., Suzuki, N., Yokoyama, F., Takaki, S., Umezawa, K., Higo, J., Mochizuki, M., Kikkawa, Y., Oishi, S., Utani, A., and Nomizu, M. (2007) Cyclic peptide analysis of the biologically active loop region in the laminin α3 chain LG4 module demonstrates the importance of peptide conformation on biological activity. *Biochemistry 46*, 1952–1960.
29. Galliano, M. F., Aberdam, D., Aguzzi, A., Ortonne, J. P., and Meneguzzi, G. (1995) Cloning and complete primary structure of the mouse laminin α3 chain. Distinct expression pattern of the laminin α3A and α3B chain isoforms. *J. Biol. Chem. 270*, 21820–21826.
30. Mochizuki, M., Kadoya, Y., Wakabayashi, Y., Kato, K., Okazaki, I., Yamada, M., Sato, T., Sakairi, N., Nishi, N., and Nomizu, M. (2003) Laminin-1 peptide-conjugated chitosan membranes as a novel approach for cell engineering. *FASEB J. 17*, 875–877.
31. Mochizuki, M., Yamagata, N., Philp, D., Hozumi, K., Watanabe, T., Kikkawa, Y., Kadoya, Y., Kleinman, H. K., and Nomizu, M. (2007) Integrin-dependent cell behavior on ECM peptide-conjugated chitosan membranes. *Biopolymers 88*, 122–130.
32. Greene, L. A., and Tischler, A. S. (1976) Establishment of a noradrenergic clonal line of rat adrenal pheochromocytoma cells which respond to nerve growth factor. *Proc. Natl. Acad. Sci. U.S.A. 73*, 2424–2428.
33. Richard, B. L., Nomizu, M., Yamada, Y., and Kleinman, H. K. (1996) Identification of synthetic peptides derived from laminin α1 and α2 chains with cell type specificity for neurite outgrowth. *Exp. Cell Res. 228*, 98–105.
34. Hoffman, M. P., Engbring, J. A., Nielsen, P. K., Vargas, J., Steinberg, Z., Karmand, A. J., Nomizu, M., Yamada, Y., and Kleinman, H. K. (2001) Cell type-specific differences in glycosaminoglycans modulate the biological activity of a heparin-binding peptide (RKRLQVQLSIRT) from the G domain of the laminin α1 chain. *J. Biol. Chem. 276*, 22077–22085.
35. Miner, J. H., Patton, B. L., Lentz, S. I., Gilbert, D. J., Snider, W. D., Jenkins, N. A., Copeland, N. G., and Sanes, J. R. (1997) The laminin α chains: Expression, developmental transitions, and chromosomal locations of α1−5, identification of heterotrimeric laminins 8−11, and cloning of a novel α3 isoform. *J. Cell Biol. 137*, 685–701.
36. Kim, J. M., Park, W. H., and Min, B. M. (2005) The PPFLMLLKGSTR motif in globular domain 3 of the human

laminin-5 α3 chain is crucial for integrin α3β1 binding and cell adhesion. *Exp. Cell Res. 304*, 317–327.
37. Okamoto, O., Bachy, S., Odenthal, U., Bernaud, J., Rigal, D., Lortat-Jacob, H., Smyth, N., and Rousselle, P. (2003) Normal human keratinocytes bind to the α3LG4/5 domain of unprocessed laminin-5 through the receptor syndecan-1. *J. Biol. Chem. 278*, 44168–44177.
38. Hozumi, K., Suzuki, N., Uchiyama, Y., Katagiri, F., Kikkawa, Y., and Nomizu, M. (2009) Chain-specific heparin-binding sequences in the laminin α chain LG45 modules. *Biochemistry 48*, 5375–5381.
39. Tashiro, K., Sephel, G. C., Weeks, B., Sasaki, M., Martin, G. R., Kleinman, H. K., and Yamada, Y. (1989) A synthetic peptide containing the IKVAV sequence from the A chain of laminin mediates cell attachment, migration, and neurite outgrowth. *J. Biol. Chem. 264*, 16174–16182.
40. Kasai, S., Urushibata, S., Hozumi, K., Yokoyama, F., Ichikawa, N., Kadoya, Y., Nishi, N., Watanabe, N., Yamada, Y., and Nomizu, M. (2007) Identification of multiple amyloidogenic sequences in laminin-1. *Biochemistry 46*, 3966–3974.
41. Hozumi, K., Suzuki, N., Nielsen, P. K., Nomizu, M., and Yamada, Y. (2006) Laminin α1 chain LG4 module promotes cell attachment through syndecans and cell spreading through integrin α2β1. *J. Biol. Chem. 281*, 32929–32940.
42. Carafoli, F., Clout, N. J., and Hohenester, E. (2009) Crystal structure of the LG1-3 region of the laminin α2 chain. *J. Biol. Chem. 284*, 22786–22792.
43. Okazaki, I., Suzuki, N., Nishi, N., Utani, A., Matsuura, H., Shinkai, H., Yamashita, H., Kitagawa, Y., and Nomizu, M. (2002) Identification of biologically active sequences in the laminin α4 chain G domain. *J. Biol. Chem. 277*, 37070–37078.
44. Grose, R., Hutter, C., Bloch, W., Thorey, I., Watt, F. M., Fassler, R., Brakebusch, C., and Werner, S. (2002) A crucial role of β1 integrins for keratinocyte migration in vitro and during cutaneous wound repair. *Development 129*, 2303–2315.